Heterogeneous Mean First-Passage Time Scaling in Fractal Media

Hyun-Myung Chun,[1] Sungmin Hwang,[2] Byungnam Kahng,[3] Heiko Rieger,[4,5] and Jae Dong Noh[6]
[1]School of Physics, Korea Institute for Advanced Study, Seoul 02455, Korea
[2]Capital Fund Management, 75007 Paris, France
[3]Center for Complex Systems Studies, and KENTECH Institute for Grid Modernization, Korea Institute of Energy Technology, Naju 58217, Korea
[4]Center for Biophysics and Department of Theoretical Physics, Saarland University, 66123 Saarbrücken, Germany
[5]Lebniz-Institute for New Materials INM, 66123 Saarbrücken, Germany
[6]Department of Physics, University of Seoul, Seoul 02504, Korea

(Received 28 April 2023; accepted 3 November 2023; published 29 November 2023)

The mean first passage time (MFPT) of random walks is a key quantity characterizing dynamic processes on disordered media. In a random fractal embedded in the Euclidean space, the MFPT is known to obey the power law scaling with the distance between a source and a target site with a universal exponent. We find that the scaling law for the MFPT is not determined solely by the distance between a source and a target but also by their locations. The role of a site in the first passage processes is quantified by the random walk centrality. It turns out that the site of highest random walk centrality, dubbed as a hub, intervenes in first passage processes. We show that the MFPT from a departure site to a target site is determined by a competition between direct paths and indirect paths detouring via the hub. Consequently, the MFPT displays a crossover scaling between a short distance regime, where direct paths are dominant, and a long distance regime, where indirect paths are dominant. The two regimes are characterized by power laws with different scaling exponents. The crossover scaling behavior is confirmed by extensive numerical calculations of the MFPTs on the critical percolation cluster in two dimensional square lattices.

DOI: 10.1103/PhysRevLett.131.227101

Introduction.—Random walks are fundamental for stochastic processes, such as transport, search, and spreading. While random walks on regular lattices have long been studied [1], there has been an ever-increasing interest in the topic incorporating structural disorder of the underlying substrate [2], geometric confinement [3], stochastic resetting [4], non-Markovian dynamics [5], and many more.

An important quantity characterizing random walks (RWs) is the first passage time (FPT) distribution and the mean first passage time (MFPT) [1,6]. Scaling properties of the FPT and MFPT reflect the interplay between the RW dynamics and geometric properties of the underlying substrate. For example, on infinite lattices, the FPT distribution follows a power law with a universal exponent [1,6]. Generally, in finite scale-invariant media, the MFPT $T(r)$ between two sites at a distance r is known to obey the scaling law [7–9]

$$T(r) \sim \begin{cases} N r^{d_w - d_f}, & \text{for } d_w > d_f \\ N \ln r, & \text{for } d_w = d_f \\ N, & \text{for } d_w < d_f \end{cases}, \tag{1}$$

where N is the total number of sites, d_f is the fractal dimension of the medium, and d_w is its walk dimension. It is remarkable that the scaling law is governed by only one universal exponent, $\theta = d_w - d_f$. On the other hand, on a highly heterogeneous graph, the MFPT displays a more complex scaling behavior [10–13]. In a scale-free network characterized by a power-law distribution of local connectivity of each site, the FPT and the MFPT averaged over source sites display a target site dependent scaling behavior [13]. Generally, in heterogeneous media, the MFPT from site i to j could be very different from the MFPT from j to i: for undirected graphs, one can assign a potential-like quantity, called the RW centrality (RWC), to each site [14]. Since the MFPT between two sites in either direction differs by the difference in their inverse RWCs (see below), a wide distribution of the RWCs could lead to a source-target specific, or heterogeneous, scaling of the MFPT, which is what we will address in this Letter.

To this purpose, we reconsider the scaling law in Eq. (1) for two-dimensional (2D) critical bond percolation clusters. We will show that despite a homogeneous local connectivity distribution, the MFPT displays a heterogeneous scaling behavior characterized by a site-dependent scaling exponent and an intriguing crossover scaling, for which the site with the highest RWC responsible. RWs on critical percolation clusters have long been studied [2,15–18], but a site-dependent or heterogeneous scaling has not been reported yet. Our Letter also sheds light on the role of the RWC for RWs in disordered media.

Random walk centrality.—We consider an undirected graph consisting of N sites, whose connectivity is represented with a symmetric adjacency matrix $\mathsf{A} = \mathsf{A}^T$, whose matrix elements A_{ij} are 0 or 1 indicating the absence or presence of an edge between sites i and j [19], respectively. The number of edges attached to a site i is its degree and is given by $k_i = \sum_j A_{ij}$. A discrete time RW on the graph is defined by the transition matrix $\mathsf{W} = \mathsf{K}^{-1}\mathsf{A}$, where K is a diagonal matrix with $K_{ij} = \delta_{ij}k_i$. That is, a random walker at site i jumps to site j with the probability $W_{ij} = A_{ij}/k_i$ in a unit time step $\Delta t = 1$. The transition matrix has the left row eigenvector $\langle \boldsymbol{\pi}| = (\pi_1, \ldots, \pi_i, \ldots, \pi_N)$ with $\pi_i = k_i/(\sum_j k_j)$ and the right column eigenvector $|\mathbf{1}\rangle = (1, 1, \ldots, 1)^T$, both with eigenvalue $\lambda = 1$. The left eigenvector corresponds to the steady state probability distribution [14].

A general theoretical framework for studying discrete time random walks has been formulated some time ago [1,14,20]. There the MFPT from site i to j is given by [14]

$$T_{ij} = \frac{R_{jj} - R_{ij} + \delta_{ij}}{\pi_j}, \tag{2}$$

where the matrix R is called the group generalized inverse of $(\mathsf{I} - \mathsf{W})$ [21,22] and given by $\mathsf{R} \equiv \sum_{t=0}^{\infty}(\mathsf{W}^t - |\mathbf{1}\rangle\langle\boldsymbol{\pi}|)$ [23]. Condamin *et al.* [7] noticed that R_{ij} is dominated by the term $\sum_{t=0}^{\infty} W(j,t|i)$, where $W(j,t|i) \equiv (\mathsf{W}^t)_{ij}$ is the probability to find the walker at site j in t steps when it started at site i. Assuming the scaling form $W(j,t|i) = t^{-d_f/d_w}\Pi(r_{ij}/t^{1/d_w})$ with r_{ij} being the Euclidean distance between i and j [2], they derived the scaling law in Eq. (1) [7].

The formal expression in Eq. (2) has a deeper implication when the transition probabilities satisfy the detailed balance condition, $\pi_i W_{ij} = \pi_j W_{ji}$ for all i and j, which holds for RWs on undirected graphs. Then, one can assign an RWC $C_i \equiv \pi_i/R_{ii}$ to each site i, relating the MFPTs T_{ij} and T_{ji} by [14]

$$T_{ij} - T_{ji} = C_j^{-1} - C_i^{-1}. \tag{3}$$

The RWC is an indicator of the attractiveness of a site in the random walk process: a first passage to a higher RWC site from a lower RWC site takes less time than the first passage in the opposite direction. The RWC has also been used to identify influential nodes in complex networks [24–28]. The inverse of the RWC $\alpha_i \equiv 1/C_i = R_{ii}/\pi_i$ is equal to the average MFPT to site i from a random departure site j sampled with the steady state probability distribution, $\alpha_i = \sum_{j\neq i}\pi_j T_{ji}$. It is also called the global mean first passage time [10,29], or the accessibility index [30]. Similarly, Kemeny's constant is defined as $K_i = \sum_{j\neq i} T_{ij}\pi_j = \sum_j R_{jj}$, which is independent of i and a characteristic of an underlying graph [20,30,31].

MFPT from hub and marginal site.—In a disordered medium site-to-site fluctuations of the RWC may affect the scaling of the MFPT with the distance. We address this issue for the RW on the critical bond percolation cluster of 2D square lattices [2,3,15–17], which we generate by occupying bonds of a 2D $L \times L$ square lattice with periodic boundary conditions with the critical occupation probability $p_c = 1/2$ and identifying the largest cluster. The 2D critical percolation cluster is a random fractal with the fractal dimension $d_f = 91/48$ [32]. The walk dimension is known to be $d_w \simeq 2.87 > d_f$ [33].

It is computationally demanding to evaluate the RWC and the MFPT for it requires to find the group generalized inverse of $\mathsf{I} - \mathsf{W}$ [26]. We will adapt the numerical algorithm developed in Ref. [34], which turns out to be extremely efficient. It takes only a few minutes in an ordinary desktop computer to compute the RWC distribution for the critical percolation cluster of lattices of size 1024×1024. All numerical data for 2D percolation clusters are obtained on a 2D lattice with $L = 1024$, if not stated otherwise, and averaged over at least 2000 independent realizations of the critical percolation cluster.

Figure 1 illustrates an RWC configuration on a critical bond percolation cluster. The RWC distribution is highly heterogeneous (see Appendix A in the Supplemental Material [35]). High RWC sites are clustered and spread out in a filamentous pattern, which is analogous to the backbone structure [2]. This heterogeneity raises questions about the simple scaling of the MFPT with a single scaling exponent as in Eq. (1).

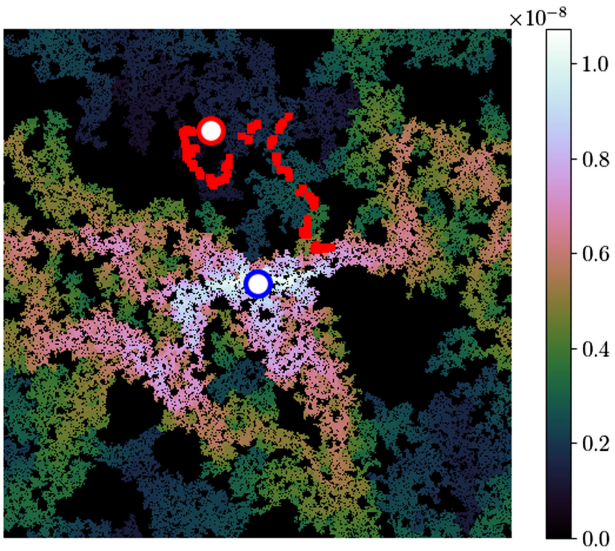

FIG. 1. RWC configuration on a 2D critical percolating cluster in a lattice of size 1024×1024. The highest and lowest RWC sites are marked with blue and red circles, respectively. Red line segments denote bridges between them (see the main text). The black area represents sites that do not belong to the percolating cluster.

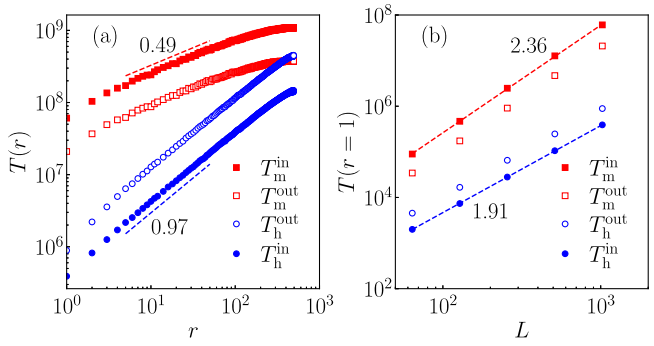

FIG. 2. (a) Average MFPT between the hub (circular symbols) or the marginal site (rectangular symbols) with the other sites. The outbound and inbound MFPTs are marked with empty and filled symbols, respectively. In (b), we plot the MFPTs from and to sites at a unit distance $r = 1$ as a function of the linear system size $64 \le L \le 1024$. The scaling exponents are obtained by fitting the data within the range indicated by the dashed lines.

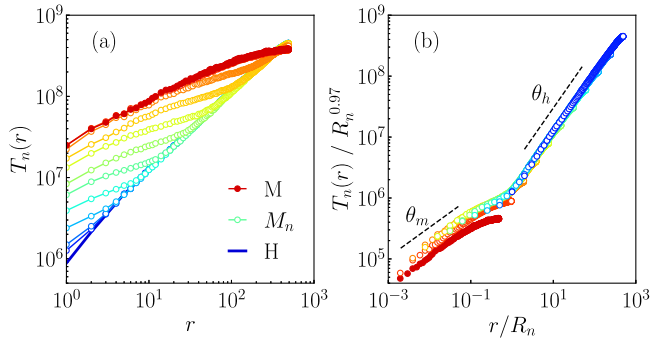

FIG. 3. (a) Outbound MFPT T_n from the site M_n (open symbols). Also shown is the MFPT from the hub (H, thick line) and the marginal site (M, filled symbols). (b) Scaling plot of $T_n(r)/R_n^{\theta_h}$ vs r/R_n with $R_n = 2^{n-1}$. The dashed lines of slope θ_h and θ_m given in Eq. (5) are guides to the eye.

To highlight the site dependence of the MFPT, we identify the *hub* (highest RWC site) and the *marginal site* (lowest RWC site), and measure the average outbound and inbound MFPTs to and from all the other sites at a given distance r. As shown in Fig. 2, the outbound MFPT is larger than the inbound MFPT for the hub, and vice versa for the marginal site. The difference is exactly given by the difference in the inverse RWCs [see Eq. (3)]. The MFPTs scale algebraically with L and r as

$$T \sim L^{\Delta} r^{\theta} \tag{4}$$

with the scaling exponents Δ and θ. Surprisingly, the hub and the marginal site are characterized by different scaling exponents

$$\theta = \begin{cases} \theta_h \simeq 0.97(5), & \text{for the hub} \\ \theta_m \simeq 0.49(5), & \text{for the marginal site.} \end{cases} \tag{5}$$

The exponent θ_h associated with the hub is close to the exponent $d_w - d_f = 0.97(4)$ of Eq. (1) in value. On the other hand, the MFPT at the marginal site grows with a considerably smaller exponent $\theta_m \simeq 0.49$ (see Appendix B in the Supplemental Material [35] for detailed analysis). The finite size scaling exponent Δ also varies. It takes on $\Delta_h \simeq 1.90$ for the hub, which is in agreement with the fractal dimension $d_f = 91/48$ of Eq. (1) [7]. The marginal site displays a stronger finite size effect with $\Delta_m \simeq 2.36 > \Delta_h$.

We note that $\Delta_h + \theta_h \simeq \Delta_m + \theta_m$. It is understood from the site independence of Kemeny's constant [30]. Kemeny's constant evaluated at a site i is given by $K_i = \sum_{j \neq i} T_{ij} \pi_j$. Since $\pi_j = a_j/N$ with $O(1)$ constant a_j, Kemeny's constant is approximated as the arithmetic average of outbound MFPTs to all the other sites. The scaling form in Eq. (4) leads to $K \sim L^{\Delta+\theta}$. Thus, $\Delta + \theta$ should be the same at the sites obeying Eq. (4). We also note that the inbound and outbound MFPTs differ by a constant factor. From now on, we focus our Letter on the outbound MFPT.

Crossover scaling of MFPT.—The site-dependent scaling behavior is not limited to an exceptional outlier site: We consider the outbound MFPTs from a set of source sites $\{M_1, M_2, \cdots\}$ selected hierarchically as follows. We select the local minimum RWC site M_n among all sites within a circle of radius $R_n = 2^{n-1}$ centered at the hub. The outbound MFPT $T_n(r)$ from M_n as a function of the distance r to target sites is shown in Fig. 3(a). We find an interesting crossover of $T_n(r)$. It grows algebraically with r with the exponent θ_m for $r \ll R_n$ and with the exponent θ_h for $r \gg R_n$. The crossover scaling behavior is summarized by the scaling form

$$T_n(r) = N R_n^{\theta_h} \mathcal{F}(r/R_n), \tag{6}$$

where the scaling function $\mathcal{F}(x)$ behaves as $\mathcal{F}(x \ll 1) \sim x^{\theta_m}$ and $\mathcal{F}(x \gg 1) \sim x^{\theta_h}$. The crossover scaling is confirmed by the scaling plot shown in Fig. 3(b). The crossover scaling persists when one chooses a source site at random among the sites at given distance from the hub (see Appendix C in the Supplemental Material [35]).

Our numerical results highlight the role of the highest RWC site in the random walk dynamics. Imagine an ensemble of the first passage events from a source site s to a target site t at a distance r_{s-t}. Let r_{s-h} be the distance from s to the hub. When the target is farther than the hub ($r_{s-t} \gg r_{h-s}$), the ensemble is dominated by the paths detouring via the hub. Consequently the MFPT follows the scaling $T \sim r^{\theta_h}$ with the scaling exponent $\theta_h = d_w - d_f$ irrespective of s. On the other hand, when the target is closer than the hub ($r_{s-t} \ll r_{h-s}$), the ensemble is dominated by direct paths and the MFPT scaling law depends on the choice of s (see Appendix D in the Supplemental Material [35]). The crossover may be overlooked when one

measures the MFPT averaged over all pairs of source and target sites at a given distance.

One can understand the origin (and potential complications) of the scaling law for $T(r)$ in Eq. (1) [7] by the following consideration: Given a source-target pair at a distance r, one partitions the entire graph into blocks of linear size $\xi_r \sim r$, putting the source and target into the same block denoted as starting block. Each block has $N_r \sim r^{d_f}$ sites and the total number of blocks is $\mathcal{N}_r \sim N/N_r \sim Nr^{-d_f}$. If all blocks were statistically equivalent, the RW would always spend $\tau_r \sim r^{d_w}$ time steps in a single block until it hops to a neighboring block. With Eq. (2) the return time to the starting block is $T_{\rm ret} \sim \tau_r \cdot (1/\pi_b)$, with the probability to be in one block $\pi_b \sim 1/\mathcal{N}_r \sim r^{d_f}/N$, thus $T_{\rm ret} \sim Nr^{d_w-d_f}$. The MFPT can then be estimated as $T_{\rm ret}/P_s$, with P_s the probability to find the target site before leaving the starting block, which is $P_s = O(1)$ for $d_w > d_f$ and $P_s \sim \tau_r/N_r \sim r^{d_w-d_f}$ for $d_w < d_f$. This argument reproduces the scaling law Eq. (1), except for the marginal case $d_w = d_f$, It clearly reveals that the simple scaling, $T(r) \sim r^{\theta}$ with a unique scaling exponent θ, is based on the assumption that the entire fractal lattice can be partitioned into homogeneous blocks. Similar arguments may also lead to scaling laws for the higher moments of the FPT distribution, cf. Ref. [36]. Our results presented in Fig. 3, however, indicate that blocks are heterogeneous on all length scales.

This heterogeneity is further evidenced by the scaling behavior of the chemical distance (number of edges in the shortest path) $l(r)$ with respect to the Euclidean distance between two sites. The average chemical distance is known to scale as $l(r) \sim r^{d_{\rm min}}$., with $d_{\rm min} \simeq 1.14$ for the 2D critical percolation cluster (Sec. 6.6 of [37]). We discriminate again between the hub (h) and the marginal site (m) as starting site and found

$$l(r) \sim \begin{cases} L^{\delta_h} r^{d_{\rm min},h}, & \delta_h \simeq 0.0, \quad d_{\rm min.,h} \simeq 1.11, \\ L^{\delta_m} r^{d_{\rm min},m}, & \delta_m \simeq 0.52, \quad d_{\rm min.,m} \simeq 0.58. \end{cases} \tag{7}$$

The chemical distance $l_n(r)$ from the local minimum RWC site M_n shows again a crossover $l_n(r) = L^{\delta_h} R_n^{d_{\rm min.,h}} \mathcal{G}(l/R_n)$ for $1 \ll R_n \ll L$. We also looked at the MFPT as a function of the chemical distance and observed a similar crossover behavior (see Appendix E in the Supplemental Material [35] for the detailed analysis for the chemical distance scaling).

Origin of crossover scaling.—A fractal may comprise a subset of sites or bonds which is itself a fractal. For instance, 2D percolation clusters contain red bonds (or cutting bonds) which themselves form a fractal with fractal dimension $d_{\rm red} = 3/4$ [38]. More generally, a percolation cluster has a mesoscale structure consisting of a backbone, red bonds, and dangling ends [2,39]. This structural heterogeneity is the origin of the site-dependent scaling and the crossover scaling.

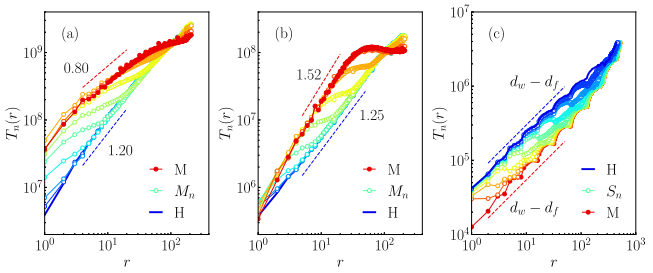

FIG. 4. Crossover scaling of the MFPT for (a) 3D critical percolation clusters, (b) 3D random walk trails, and (c) the Sierpiński gasket.

To support this claim, we study the distribution of *bridges* [40] between the hub and the marginal site in 2D percolation clusters. A bond is defined to be a bridge if the marginal site would be disconnected from the hub without it, represented by red lines in Fig. 1 [41]. We find that the total number of bridges obeys the power law scaling $N_{\rm b} \sim L^{0.75}$ (see Appendix F in the Supplemental Material [35]), which indicates that the marginal site is located deep within a dangling end. Moreover, as Fig. 1 illustrates, bridges are predominantly distributed near the marginal site. Consequently, random walks from the marginal site are *quasi-one-dimensional* along a path consisting mainly of the bridges. The MFPT from a marginal site to another separated by a chemical distance l then scales like the 1D random walk MFPT $T(l) \sim Nl^1$. Since the chemical distance l scales with the Euclidean distance r as given in Eq. (7), we obtain

$$T(r) \sim L^{d_f+\delta_m} r^{d_{\rm min},m}. \tag{8}$$

Note that $d_f + \delta_m \simeq 2.42$ and $d_{{\rm min},m} \simeq 0.58$, which are close to $\Delta_m \simeq 2.36$ and $\theta_m \simeq 0.49$, respectively [cf. Eq. (5)]. Our argument reveals that the quasi-one-dimensional structure of bridges near the marginal site is responsible for the crossover scaling. It also predicts, at least approximately, the scaling exponents Δ_m and θ_m in terms of the geometric quantities δ_m and $d_{{\rm min},m}$.

We performed similar studies for 3D percolation clusters [42], random walk trails [43], and the Sierpiński gasket. We observe the described crossover scaling for the random fractals as shown in Fig. 4. We point out that for the deterministic fractal shown here (Sierpiński gasket), the scaling exponents are site independent (see Appendix G in the Supplemental Material [35] for further discussion).

Conclusion.—We report in this Letter, for the first time, heterogeneous scaling behavior of the MFPT of RWs on a random fractal, the critical percolation cluster in 2D. MFPTs measured from the hub and measured from the marginal site as a function of the distance of the target site obey power law scaling with distinctively different exponents and the distance dependence of MFPTs from general starting sites shows a striking crossover.

Heterogeneous behavior of various observables in disordered systems is expected, as, for instance, dynamical heterogeneities in glassy systems [44] or in the context of Griffiths singularities in strongly disordered systems [45] like the transverse Ising chain [46] or the Sinai walk [47]. A lack of self-averaging is a prominent consequence of this spatial heterogeneity [48], and it manifests itself in the quantities we looked at. But different power laws for different regions in the system, as we find them for regions close to the hub and close to the marginal site, have, to our knowledge, not been reported before. An important consequence of our results is that scaling theories for the MFPT that are based on an explicit or hidden spatial homogeneity assumption should be considered more carefully.

The origin of the strong heterogeneity in the MFPT can be traced back to the broad distribution of the RWC. Our results could be generalized to, and are relevant for, a larger class of heterogeneous media embedded in real space, like diffusion-limited aggregation, random resistor networks, lattice animals, and so on. We also speculate that heterogeneous scaling could occur in multifractal systems characterized by a continuous spectrum of fractal dimension. Our results also suggest that the RWC distribution is important to understand information spreading dynamics on complex networks.

J. D. N was supported by the National Research Foundation of Korea (NRF) grant funded by the Korea government (MSIP) (Grants No. 2019R1A2C1009628). H. R. acknowledges financial support by the German Research Foundation (DFG) within the Collaborative Research Center SFB 1027-A3 and INST 256/539-1. H.-M. C. was supported by a KIAS Individual Grant (PG089401) at Korea Institute for Advanced Study. B. K. was supported by the National Research Foundation of Korea by Grants No. NRF-2014R1A3A2-069005 and No. RS-2023-00279802 and the KENTECH Research Grant No. KRG-2021-01-007.

[1] B. D. Hughes, *Random Walks and Random Environments. Volume 1: Random Walks* (Clarendon Press, Oxford, 1995).
[2] S. Havlin and D. Ben-Avraham, Diffusion in disordered media, Adv. Phys. **51**, 187 (2002).
[3] O. Bénichou, C. Chevalier, J. Klafter, B. Meyer, and R. Voituriez, Geometry-controlled kinetics, Nat. Chem. **2**, 472 (2010).
[4] M. R. Evans, S. N. Majumdar, and G. Schehr, Stochastic resetting and applications, J. Phys. A **53**, 193001 (2020).
[5] A. Barbier-Chebbah, O. Bénichou, and R. Voituriez, Self-interacting random walks: Aging, exploration, and first-passage times, Phys. Rev. X **12**, 011052 (2022).
[6] S. Redner, *A Guide to First-Passage Processes* (Cambridge University Press, New York, 2001).
[7] S. Condamin, O. Bénichou, V. Tejedor, R. Voituriez, and J. Klafter, First-passage times in complex scale-invariant media, Nature (London) **450**, 77 (2007).
[8] S. Reuveni, R. Granek, and J. Klafter, Vibrational shortcut to the mean-first-passage-time problem, Phys. Rev. E **81**, 040103(R) (2010).
[9] A. P. Roberts and C. P. Haynes, Electrostatic approximation of source-to-target mean first-passage times on networks, Phys. Rev. E **83**, 031113 (2011).
[10] V. Tejedor, O. Bénichou, and R. Voituriez, Global mean first-passage times of random walks on complex networks, Phys. Rev. E **80**, 065104(R) (2009).
[11] E. Agliari, R. Burioni, and A. Manzotti, Effective target arrangement in a deterministic scale-free graph, Phys. Rev. E **82**, 011118 (2010).
[12] V. Tejedor, O. Bénichou, and R. Voituriez, Close or connected: Distance and connectivity effects on transport in networks, Phys. Rev. E **83**, 066102 (2011).
[13] S. Hwang, D. S. Lee, and B. Kahng, First passage time for random walks in heterogeneous networks, Phys. Rev. Lett. **109**, 088701 (2012).
[14] J. D. Noh and H. Rieger, Random walks on complex networks, Phys. Rev. Lett. **92**, 118701 (2004).
[15] J. C. A. d'Auriac, A. Benoit, and R. Rammal, Random walk on fractals: Numerical studies in two dimensions, J. Phys. A **16**, 4039 (1983).
[16] S. Alexander and R. Orbach, Density of states on fractals: ≪ fractons ≫, J. Phys. Lett. **43**, 625 (1982).
[17] O. Bénichou, B. Meyer, V. Tejedor, and R. Voituriez, Zero constant formula for first-passage observables in bounded domains, Phys. Rev. Lett. **101**, 130601 (2008).
[18] S. Condamin, V. Tejedor, R. Voituriez, O. Bénichou, and J. Klafter, Probing microscopic origins of confined subdiffusion by first-passage observables, Proc. Natl. Acad. Sci. U.S.A. **105**, 5675 (2008).
[19] The formalism in the Letter is also valid in a weighted graph with nonbinary adjacency matrix elements.
[20] J. G. Kemeny and J. L. Snell, *Finite Markov Chains* (Springer, New York, 1976).
[21] C. D. Meyer, Jr, The role of the group generalized inverse in the theory of finite Markov Chains, SIAM Rev. **17**, 443 (1975).
[22] J. J. Hunter, The role of Kemeny's constant in properties of Markov Chains, Commun. Stat. **43**, 1309 (2014).
[23] The matrix $(\mathsf{I}-\mathsf{W})$ is not invertible because one of the eigenvalues of W equals to 1. The group generalized inverse is defined as $\sum_{n=2}^{N}[1/(1-\lambda_n)]|\lambda_n\rangle\langle\lambda_n|$, where λ_n, $|\lambda_n\rangle$, $\langle\lambda_n|$ are the nth eigenvalue, right eigenvector, and left eigenvector of W, respectively. The sum excludes the eigenstate with $\lambda_1 = 1$.
[24] M. Loecher and J. Kadtke, Enhanced predictability of hierarchical propagation in complex networks, Phys. Lett. A **366**, 535 (2007).
[25] F. Blöchl, F. J. Theis, F. Vega-Redondo, and E. O. Fisher, Vertex centralities in input-output networks reveal the structure of modern economies, Phys. Rev. E **83**, 046127 (2011).
[26] B. C. Johnson and S. Kirkland, Estimating random walk centrality in networks, Comput. Stat. Data Anal. **138**, 190 (2019).
[27] S. Oldham, B. Fulcher, L. Parkes, A. Arnatkevičiūtė, C. Suo, and A. Fornito, Consistency and differences between

centrality measures across distinct classes of networks, PLoS One **14**, e0220061 (2019).
[28] A. P. Riascos, D. Boyer, P. Herringer, and J. L. Mateos, Random walks on networks with stochastic resetting, Phys. Rev. E **101**, 062147 (2020).
[29] Z. Zhang, Y. Qi, S. Zhou, S. Gao, and J. Guan, Explicit determination of mean first-passage time for random walks on deterministic uniform recursive trees, Phys. Rev. E **81**, 016114 (2010).
[30] S. Kirkland, Random walk centrality and a partition of Kemeny's constant, Czech. Math. J. **66**, 757 (2016).
[31] S. Yilmaz, E. Dudkina, M. Bin, E. Crisostomi, P. Ferraro, R. Murray-Smith, T. Parisini, L. Stone, and R. Shorten, Kemeny-based testing for COVID-19, PLoS One **15**, e0242401 (2020).
[32] D. Stauffer and A. Aharony, *Introduction to Percolation Theory*, 2nd ed. (Taylor & Francis, London, 1992).
[33] I. Majid, D. Avraham, S. Havlin, and H. E. Stanley, Exact-enumeration approach to random walks on percolation clusters in two dimensions, Phys. Rev. B **30**, 1626 (1984).
[34] S. Hwang, D.-S. Lee, and B. Kahng, Fast algorithm for relaxation processes in big-data systems, Phys. Rev. E **90**, 043303 (2014).
[35] See Supplemental Material at http://link.aps.org/supplemental/10.1103/PhysRevLett.131.227101 for detailed discussion and addition numerical data.
[36] N. Levernier, O. Bénichou, T. Guérin, and R. Voituriez, Universal first-passage statistics in aging media, Phys. Rev. E **98**, 022125 (2018).
[37] D. Ben-Avraham and S. Havlin, *Diffusion and Reactions in Fractals and Disordered Systems* (Cambridge University Press, Cambridge, England, 2000).
[38] A. Coniglio, Cluster structure near the percolation threshold, J. Phys. A **15**, 3829 (1999).
[39] H. J. Herrmann, D. C. Hong, and H. E. Stanley, Backbone and elastic backbone of percolation clusters obtained by the new method of 'burning', J. Phys. A **17**, L261 (1999).
[40] R. Tarjan, A note on finding the bridges of a graph, Inf. Proc. Lett. **2**, 160 (1974).
[41] The bridges correspond to red bonds between the hub and the marginal site. Imagine that all bonds are identical resistors and a voltage drop is applied between the hub and the marginal site. The bridge bonds carry all current in such an electric circuit, and the current stops flowing when any of them are removed.
[42] C. D. Lorenz and R. M. Ziff, Precise determination of the bond percolation thresholds and finite-size scaling corrections for the sc, fcc, and bcc lattices, Phys. Rev. E **57**, 230 (1998).
[43] K. J. Falconer, *The Geometry of Fractal Sets* (Cambridge University Press, Cambridge, England, 1985).
[44] W. Kob, C. Donati, S. J. Plimpton, P. H. Poole, and S. C. Glotzer, Dynamical heterogeneities in a supercooled Lennard-Jones liquid, Phys. Rev. Lett. **79**, 2827 (1997); W. K. Kegel and Blaaderen, and Alfons van, Direct observation of dynamical heterogeneities in colloidal hard-sphere suspensions, Science **287**, 290 (2000).
[45] F. Iglói and C. Monthus, Strong disorder RG approach of random systems, Phys. Rep. **412**, 277 (2005).
[46] D. S. Fisher, Random transverse field Ising spin chains, Phys. Rev. Lett. **69**, 534 (1992); D. S. Fisher, Critical behavior of random transverse-field Ising spin chains, Phys. Rev. B **51**, 6411 (1995); F. Iglói and H. Rieger, Random transverse Ising spin chain and random walks, Phys. Rev. B **57**, 11404 (1998).
[47] D. S. Fisher, P. L. Doussal, and C. Monthus, Random walks, reaction-diffusion, and nonequilibrium dynamics of spin chains in one-dimensional random environments, Phys. Rev. Lett. **80**, 3539 (1998); F. Iglói and H. Rieger, Anomalous diffusion in disordered media and random quantum spin chains, Phys. Rev. E **58**, 4238 (1998).
[48] A. Aharony and A. B. Harris, Absence of self-averaging and universal fluctuations in random systems near critical points, Phys. Rev. Lett. **77**, 3700 (1996); S. Wiseman and E. Domany, Finite-size scaling and lack of self-averaging in critical disordered systems, Phys. Rev. Lett. **81**, 22 (1998).